Power Amplification at THz via Plasma Wave Excitation in RTD-Gated HEMTs

Berardi Sensale-Rodríguez, *Student Member, IEEE*, Lei Liu, *Member, IEEE*, Patrick Fay, *Senior Member, IEEE*, Debdeep Jena, *Member, IEEE*, and Huili Grace Xing, *Member, IEEE*

***Abstract*—We report studies of amplification arising from the dynamics of electron plasma waves in a high electron mobility transistor (HEMT) channel with injection from the gate exhibiting negative differential conductance (NDC). The gate NDC can be realized in a resonant tunnel diode (RTD) gate structure integrated in the HEMT. Though the electron plasma wave by itself cannot enable amplification, when coupled with gate NDC, they together form a gain medium at terahertz (THz) frequencies due to the higher plasma wave group velocity than the electron drift velocity. The analysis is developed using a distributed circuit model based on the Dyakonov–Shur hydrodynamic theory. Numerical and analytical results suggest that these devices can realize power amplification with a gain exceeding 5 dB while simultaneously providing conditional stability at THz frequencies.**

***Index Terms*—Amplification, gain, high electron mobility transistor (HEMT), negative differential conductance (NDC), plasma, resonant tunnel diode (RTD), terahertz (THz).**

I. Introduction

The past decades have seen increasingly rapid advances in the field of terahertz (THz) research [1]. However, in spite of these efforts, obtaining power amplification at THz frequencies has remained a significant challenge. In this work, we theoretically explore, based on Dyakonov and Shur's theory [2], [3], the possibility of THz power amplification via excitation of collective electron motion (plasma waves) in high electron mobility transistors (HEMTs) in conjunction with current injection from a gate electrode exhibiting negative differential conductance (NDC). Dyakonov and Shur's theory is based on the assumption that electrons confined in the HEMT channel behave as a two-dimensional electron fluid (2DEF) and thus can be described by a hydrodynamic model, which allows excitation of plasma waves in the channel. For a typical 2D electron concentration in a micro/nanoscale HEMT, the plasma wave characteristic frequency falls in the THz band. Since the group velocity of plasma waves, generally $> 1 \times 10^8$ cm/s, is larger than the electron drift velocity, on the order of 2×10^7 cm/s, plasma wave based media is attractive for THz electronics (e.g., a transit time across 100 nm is 0.1 ps assuming an electron velocity of 1×10^8 cm/s). Several studies have shown that this phenomenon may lead to efficient detection, generation, and frequency multiplication of THz radiation; experimental demonstrations of detectors using Si- [4], GaAs- [5], and GaN-based [6] transistors, and THz emission from InGaAs–AlInAs [7] and AlGaN–GaN HEMTs [8] has been reported. In this context, previous theoretical and experimental studies have demonstrated that gate leakage current is a key parasitic that reduces the responsivity when these devices are used as detectors [9], [10]. The root cause of this degradation in device performance is increased damping of the plasma waves due to the (positive) gate conductance. During the preparation of this manuscript, we discovered Ryzhii *et al.* had earlier proposed that, in HEMTs with gates exhibiting NDC, the detector responsivity could be enhanced [11] and THz emission could be possible [12]. Indeed, the NDC can counteract the plasma damping thus enhancing detector response, which has also been shown in our recent work [13]. In this work we show that significant stable power gain at THz frequencies can be achieved via plasma-wave excitation in HEMTs with NDC gates, which can in practice be realized using resonant tunnel diode (RTD) structures integrated into the gate stack. Such devices may be considered to be RTD-gated plasma-wave HEMTs.

Another added advantage of the proposed device is that optical phonon emission and absorption do not play a role in the operation of the RTD-gated plasma wave HEMT discussed here, while these phenomena can limit electron drift velocity under high electric field in conventional HEMTs [14]. This distinction arises because in the RTD-gated plasma wave HEMT described here the energy difference between source and drain during operation is on the order of a few meV, much smaller than the optical phonon energy [13]. In addition, because the optical phonon energy is much greater than the photon energy in the THz, phonon generation by absorption from the THz signal frequencies is also insignificant [11].

II. Modeling

To describe a metal-gate/insulator/2DEF structure at high frequencies, a transmission line model was explicitly employed by Burke *et al.* in 2000 [15]. This model was later adopted by Khmyrova *et al.* to analyze electron-plasma-wave-based HEMTs as THz detectors [16]. In this paper, to facilitate the power amplifier design, a distributed circuit model has been built on this prior work to represent the contribution of 2DEF and NDC to the device operation in an RTD-gated plasma-wave

Manuscript received June 06, 2012; revised October 17, 2012; accepted December 13, 2012. Date of publication January 23, 2013; date of current version February 27, 2013. This work was supported in part by the Office of Naval Research under Contract N00014-11-10721, the National Science Foundation under Grant CAREER ECCS-084910 and Grant ECCS-1002088, the Center for Advanced Diagnostics and Therapeutics (AD&T), and the Center for Nanoscience and Technology (NDnano) at the University of Notre Dame.

The authors are with the Department of Electrical Engineering, University of Notre Dame, Notre Dame, IN 46556 USA (e-mail: bsensale@nd.edu; hxing@nd.edu).

Color versions of one or more of the figures in this paper are available online at http://ieeexplore.ieee.org.

Digital Object Identifier 10.1109/TTHZ.2012.2235909

2156-342X/$31.00 © 2013 IEEE

HEMT. As shown in Fig. 1(a), this distributed circuit model is analogous to that of a transmission line with the following parameters:

$$r = \frac{1}{e\mu n_s W} \quad l = \frac{m^*}{e^2 n_s W} \quad c = c_0 W \quad g = g_0 W \tag{1}$$

where r represents the distributed channel resistance, l is the kinetic inductance (accounting for the inertia of electrons in the 2DEF), and c and g represent the distributed gate capacitance and conductance, respectively. Other parameters presented in (1) are: e and m^*, the electron charge and effective mass; μ, the electron mobility in the channel; W, the transistor width; n_s, the 2DEF sheet charge density; c_0, the gate capacitance per unit area; and g_0, the gate conductance per unit area. When compared with the conventional lumped-element equivalent circuit of a HEMT shown in Fig. 1(c), one can see that the fundamental departures from conventional HEMT models in the RTD-gated plasma wave HEMT model are: 1) to replace the voltage-controlled current source (reduced to a variable resistor in the HEMT's linear I–V region) with a distributed channel resistance and kinetic inductance and 2) to replace the positive gate conductance (leakage) with a negative gate conductance (injection). In (1), the quantities n_s, c_0, and g_0—all of which are normalized to the gate area—are dependent on the HEMT bias conditions, which can be calculated using the conventional HEMT and RTD theory.

In the small-signal regime, in which the ac THz signals do not significantly alter the transistor dc operation point, one can define a transmission line propagation constant and characteristic impedance as

$$\gamma = \sqrt{(r + j\omega l)(g + j\omega c)} \quad Z = \sqrt{\frac{(r + j\omega l)}{(g + j\omega c)}} \tag{2}$$

where $\omega = 2\pi f$ is the THz angular frequency.

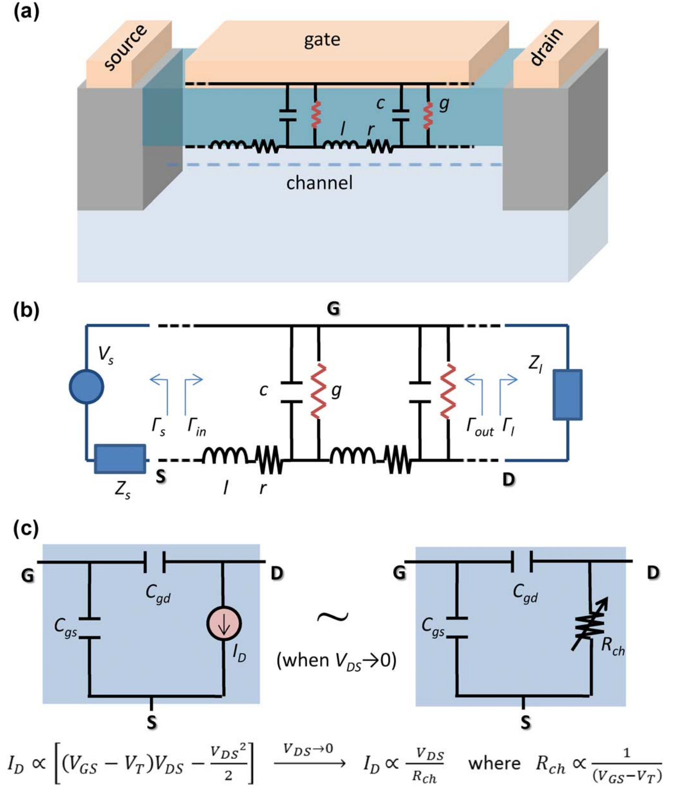

Fig. 1. (a) Distributed circuit model for an RTD-gated plasma wave HEMT, featuring an active transmission line for the channel and the gate NDC being denoted in red. (b) Equivalent circuit for analysis of the device as an amplifier: V_s and Z_s together represent the input signal source, Z_l represents the impedance of the load. (c) The conventional lumped-element equivalent circuit of an HEMT, shown for comparison.

III. Discussion

For the common-gate HEMT configuration depicted in Fig. 1(b), V_s and Z_s together represent the signal source providing the THz input excitation to the device (between source and gate), and Z_l represents the impedance of a load (between drain and gate). The device is biased such that a dc voltage is applied between gate and source, while the drain is left open-circuited at dc. Under these conditions, a small dc voltage is induced between source and drain due to operation of the device as a detector [3]. In order to simplify the analysis, this self-bias is assumed to have a negligible effect on the carrier concentration, mobility, and time-averaged electron velocity that are established by the (large-signal) dc operating conditions. Of particular interest is the situation where the gate of the HEMT exhibits NDC under the applied bias conditions, as could be realized by co-integrating an RTD into the gate stack [17]. In order to illustrate the origin of gain in these devices, two cases are analyzed: 1) real source/load impedances are assumed since analytical forms can be derived under this assumption and 2) complex source/load impedances are considered and optimized for stable power gain using numerical procedures.

For the first case, we consider a scenario where both the source and load impedances are real and equal, $Z_{s,l} = Z_s = Z_l$. Without considering stability, the transducer power gain (G_T) [18] for this configuration is given by

$$G_T = 4\left|2\cosh(\gamma L) + \sinh(\gamma L)\left(\frac{Z}{Z_{s,l}} + \frac{Z_{s,l}}{Z}\right)\right|^{-2} \tag{3}$$

where L is the HEMT channel transmission line length (for simplicity of the analysis, we treat HEMTs with self-aligned gates so that the gate overlaps the entire length of the channel between source and drain). For the case that $g = -rc/l$ and $f = f_0 = (1/(2\pi\sqrt{lc}))\sqrt{(\pi/2L)^2 - rg}$, where the quantity under the square root is considered to be positive, (3) reduces to

$$G_T = 4\left|(\xi + \xi^{-1})\right|^{-2} \tag{4}$$

where the complex quantity ξ is defined as the ratio of the plasma-wave-transmission-line impedance over the source impedance: $\xi = (Z/Z_{s,l})$. This situation corresponds to a case where the damping of the plasma waves is completely counteracted by the gate NDC. The contribution of the gate NDC does not end here, however.

As can be seen in (2), the gate NDC also strongly influences the qualitative behavior of the HEMT channel characteristic impedance Z, which is a fundamental factor to provide power gain under these circumstances. It can be observed, by inspecting (2) and (4), that NDC $(g < 0)$ is a necessary condition to achieve power gain $(G_T > 1)$. Furthermore, in order to ensure at least 6 dB of power gain from source to load, the

following condition must be satisfied: $0 < (\omega l/r) < (1/\sqrt{3})$, which can be rewritten as: $f < (1/(2\pi\sqrt{3}\tau)) = f_m$, where τ is the momentum relaxation time of electrons in the channel. The upper bound on frequency for which $G_T \geq 6$ dB, f_m, is also derived from (2) and (4). It is interesting to notice that this upper frequency depends on only one parameter, τ, e.g., $f_m \sim 0.7$ THz in GaN, when $\tau \approx 0.13$ ps. This constraint on the frequency is necessary to ensure that the power gain exceeds 6 dB under the condition of real source and load impedances $Z_s = Z_l$; for a frequency $f < f_m$, there always exists non-null real source and load impedances $Z_{s,l}$ for which $G_T > 6$ dB.

From this discussion, one can see that it is not possible to obtain significant power gain above f_m when real source/load impedances are used. To explore the possibility of obtaining stable power gain at frequencies above f_m, the case of generalized complex source and load impedances are evaluated in the second case studied in this work. In this situation, the transducer power gain is given by [18]

$$G_T = \frac{|S_{21}|^2 \left(1 - |\Gamma_s|^2\right) \left(1 - |\Gamma_l|^2\right)}{|1 - \Gamma_s \Gamma_{in}|^2 |1 - S_{22}\Gamma_l|^2} \tag{5}$$

where

$$\begin{cases} S_{11} = S_{22} = \frac{\zeta \sinh(\gamma L) - \zeta^{-1} \sinh(\gamma L)}{2\cosh(\gamma L) + \sinh(\gamma L)(\zeta + \zeta^{-1})} \\ S_{12} = S_{21} = \frac{2}{2\cosh(\gamma L) + \sinh(\gamma L)(\zeta + \zeta^{-1})} \end{cases} \tag{6}$$

and $\Gamma_{in} = S_{11} + S_{12}S_{21}\Gamma_l/(1 - S_{22}\Gamma_l)$. As can be seen in (5) and (6), G_T is a function of four complex variables: ζ, γL, Γ_s, and Γ_l, where Γ_s and Γ_l are the source and load reflection coefficients with respect to $Z_0 = 50\ \Omega$, respectively. In (6), ζ is defined as $\zeta = Z/Z_0$. Because the S parameter matrix [(6)] is symmetric (since V_{DS} is small and thus the device exhibits drain–source symmetry), Γ_s and Γ_l are interchangeable in (5), and therefore $\Gamma_s = \Gamma_l$ is satisfied in any optimal device configuration that maximizes power gain.

In view of the fact that there is no simple expression to represent (5), and since the power gain and stability are expected to be strongly dependent on the choice of source/load impedance (as previously observed for the case of detectors with arbitrary load impedances [16]), numerical optimization was performed using the methods described in [19] to obtain the impedances and device dimensions leading to maximum power gain. Meanwhile, to ensure conditional stability [18], [20], the optimization was constrained to require that $|\Gamma_{in}| < 1$ and $|\Gamma_{out}| < 1$ [where Γ_{in} and Γ_{out} are the input and output reflection coefficients as shown in Fig. 1(b)].

The material system considered for this optimization was GaN. The material and device parameters used [21], and the results of the analysis in terms of gain, stability, and optimized device properties, dimensions, and source–load impedances are presented in Table I. Optimization for gain at 2 and 4 THz was performed. It was assumed that $g = -0.9rc/l$ because gain increases with the absolute value of g and is maximized as g approaches $-rc/l$ (see Fig. 4). The maximum transducer power gain was found to be around 5.2 and 4.85 dB at 2 and 4 THz, respectively.

Transducer power gain of the optimized configuration using the parameters in Table I, with and without NDC, is presented as a function of frequency in Fig. 2(a) and (b). As illustrated in these figures, there is no power gain without NDC ($g = 0$), but the calculated G_T with and without NDC exhibits the same underlying periodicity due to the plasma waves. Thus, excitation of plasma waves is not a mechanism that can lead to power gain by itself. Also plotted in Fig. 2(a) and (b) is the power gain (G_T) considering two real-valued impedance values: $Z_{s,l} = 10\ \Omega$ and $Z_{s,l} = 50\ \Omega$. It is confirmed that, under these boundary conditions, gain is not possible at high frequencies ($f \gg f_m$), as predicted in the first case studied above, while it is possible to achieve $G_T > 6$ dB at frequencies below f_m with certain choices of $Z_{s,l}$. Hence, selection of appropriate source–load impedances is critical for achieving power gain at THz frequencies.

TABLE I
DEVICE PARAMETERS AND OPTIMIZATION RESULTS FOR ARBITRARY SOURCE–LOAD IMPEDANCES*

	2 THz	4 THz
n_s (10^{12}cm^{-2})	2.66	2.30
C (μF/cm^2)	0.69	0.69
m^*	0.2 m_0	0.2 m_0
μ (cm^2/V.s)	1400	1400
W (μm)	18	10.75
L (nm)	190	103
Re(Z_s) = Re(Z_l) (Ω)	22.5	17.3
Im(Z_s) = Im(Z_l) (Ω)	36.1	43.9
$\|\Gamma_{in}\| = \|\Gamma_{out}\|$	0.95	0.95
$\|G_T\|$ (dB)	5.20	4.85
3dB BW (GHz)	180	324

* Assuming $g = -0.9\ rc/l$.

The input/output reflection coefficient of an RTD-gated plasma wave HEMT optimized for 4-THz amplification is plotted in Fig. 3(a). One can see that the input and output reflection coefficients ($\Gamma_{\rm in}, \Gamma_{\rm out}$) are subunity over a broad interval around the operating frequency, indicating stable amplifier operation. In order to show more details regarding the influence of the source and load impedances on power gain, Fig. 3(b) shows a false-color polar plot of G_T, with constant input and output reflection coefficient contours superimposed (note that symmetry causes $|\Gamma_{\rm out}| = |\Gamma_{\rm in}|$), as a function of source and load impedance ($\Gamma_s = \Gamma_l$). The contour levels shown for $|\Gamma_{\rm out}|$ and $|\Gamma_{\rm in}|$ are 0.85, 0.9, 0.95, and 1. The regions inside the $|\Gamma_{\rm out,in}| = 1$ circles are stable. It can be observed that, for each circle representing constant output reflection coefficient, there is a specific source impedance that maximizes the power gain.

To summarize, the origin of this significant and stable power gain at THz frequencies is the interplay between the gate NDC and the fast electron-plasma waves in the channel, acting collectively as a gain medium, as well as the appropriate selection of the device dimensions and source/load impedances. Further increase in usable gain could be potentially achieved by connecting several of these devices in a distributed amplifier configuration (see, e.g., [22]). These devices might also be used as THz emitters if designed to be unstable, consistent with the proposal of Ryzhii *et al.* [12]

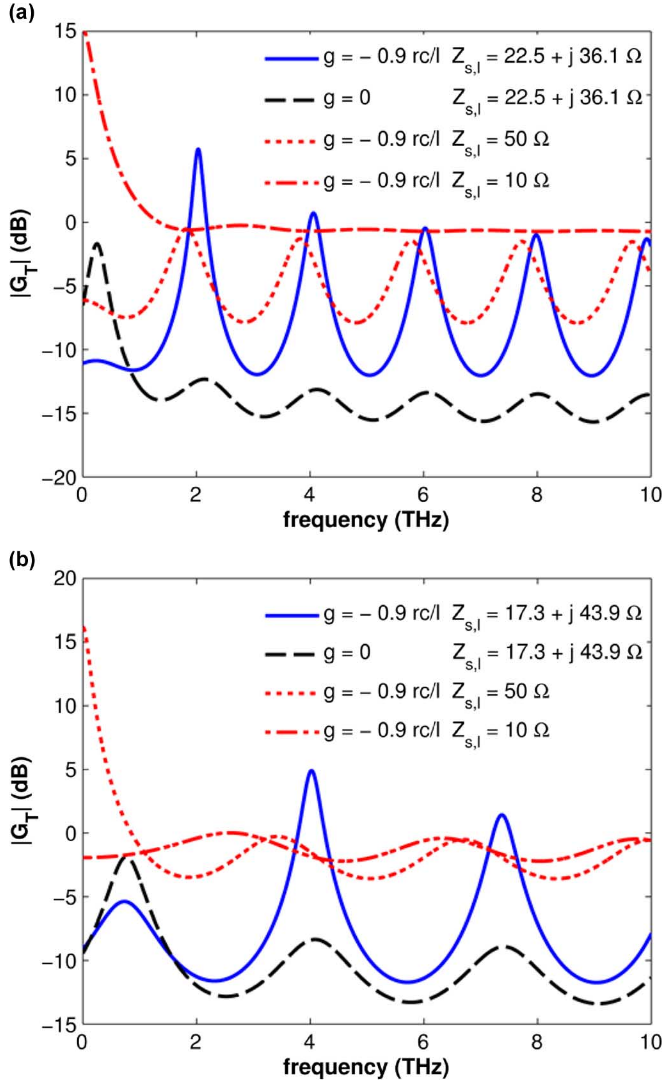

Fig. 2. Transducer power gain as a function of frequency using the parameters in Table I, with variations as noted in the legend. (a) Design for maximum gain at 2 THz. (b) Design for maximum gain at 4 THz.

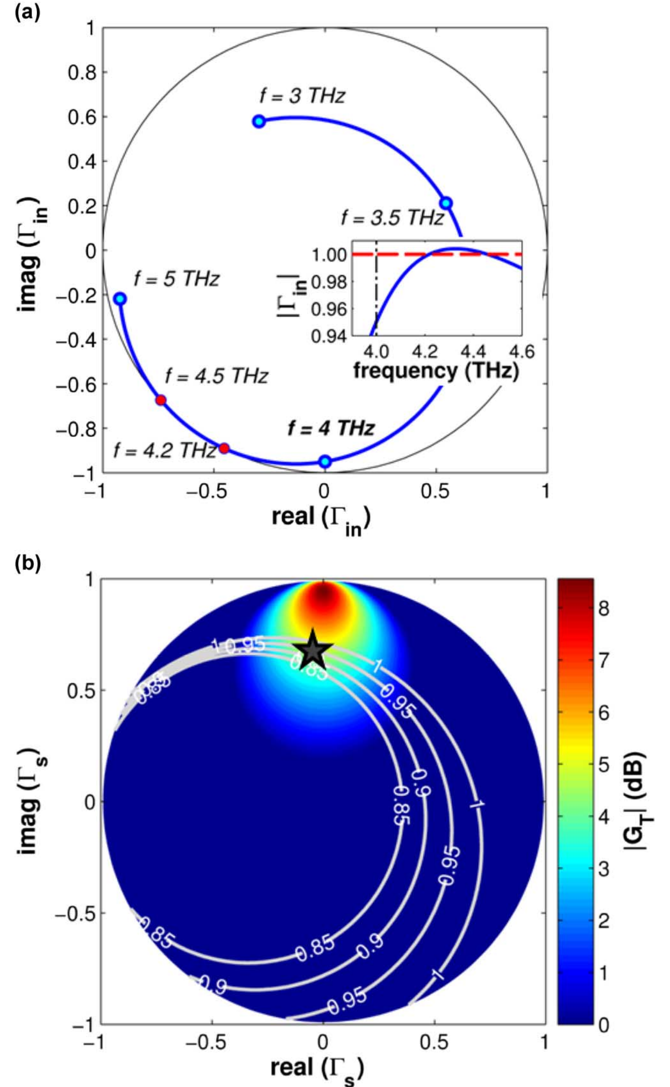

Fig. 3. Plots of the RTD-gated plasma wave HEMT amplification response, using design parameters to maximize gain at 4 THz. (a) Input (and output, due to bilateral symmetry) reflection coefficient versus frequency. Between 4.2 and 4.5 THz (red dots), the reflection coefficient is located outside the unity circle. (b) Color map of gain and circles of constant input and output reflection coefficient (white circles represent constant $|\Gamma_{in}|$ $(= |\Gamma_{out}|)$ contours for $|\Gamma_{in}| = 0.85$, 0.9, 0.5, and 1), versus real and imaginary part of Γ_s at 4 THz. In both plots, since the device has bilateral symmetry and $\Gamma_s = \Gamma_l$, the output (Γ_{out}) and input ($\Gamma_{\rm in}$) reflection coefficients are the same. The region inside the $|\Gamma_{\rm out,in}| = 1$ circle is stable. The optimized design (Table I) is depicted with a black star.

IV. Practical Considerations

To gain insight into the feasibility of practical implementation of devices based on the proposed THz amplification approach, numerical simulations of GaN-channel HEMTs with AlGaN–GaN/AlGaN RTD structures integrated in the gate (to provide NDC) were performed. Since the NDC (g) has to be of the same order as $-rc/l$ in order to achieve substantial amplification (see Fig. 4), the gate capacitance and the NDC of the RTD gate should satisfy the following condition: $|c/g| \sim \tau$, since $g \sim -rc/l = -ce/\mu\text{m}^* = -c/\tau$ according to (1) and noting that, by definition, $\tau = \mu\text{m}^*/e$. To investigate the potential for satisfying these mutual requirements for gate NDC and capacitance in practical devices, these two parameters (c and g) were estimated from conduction-band profiles and charge distributions for candidate heterostructures, as computed using a self-consistent 1-D Poisson solver [23] at various applied voltages in RTD-gated HEMTs. One example device heterostructure, together with its energy band diagram, is depicted in Fig. 5(a).

The gate current as a function of gate voltage of the RTD-gated HEMT structure was calculated using the transfer matrix formalism, where transmission probability and thus tunneling current was determined using the method described in [24]. The differential conductance was found from the derivative of current with respect to gate voltage. Several structures with different barrier/well widths and barrier height (Al composition) were simulated. From these results, it was observed that ∼1 nm barrier thicknesses with Al composition ∼25% are the most appropriate to satisfy the requirement of $|c/g| \sim \tau$. Plots of gate current and gate conductance for the example structure shown in Fig. 5(a) are given in Fig. 5(b) and (c). At the bias corresponding to the negative peak in g, $|c/g|$ was determined to be

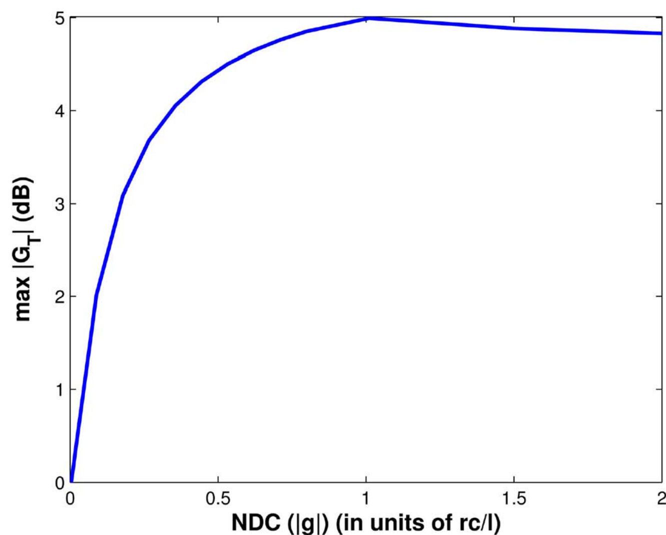

Fig. 4. Maximum stable power gain as a function of NDC at 4 THz. At each value of $|g|$, the device was optimized for maximum gain.

around 0.04 ps ($< \tau = 0.13$ ps). Even though the calculated capacitance from the 1-D Poisson solver may be underestimated under the resonant tunneling conditions [25], the requirement of $|c/g| \sim \tau$ can be satisfied. These results show that THz amplification (and also highly sensitive THz detection) appears possible in these RTD-gated plasma wave HEMTs with physically realizable heterostructure designs.

Generally speaking, realization of high-speed electronics is greatly complicated by the parasitics associated with the active device fabrication and layout. To this end, we attempt to provide a crude estimate here on the impact of parasitics on the proposed device concept for THz amplifiers. The current start-of-the-art for contact resistance reproducibly achieved in GaN HEMTs is <0.1 Ω-mm using a regrown ohmic technique [26], [27]. Using the device geometries listed in Table I and assuming a moderate sheet resistance of 400 Ω/square and 50-nm SiO_2 spacer between the ohmic regions and the gate, a parasitic source and drain access resistance of approximately 6.7 Ω can be expected for the device optimized for 2 THz operation and 11.2 Ω for the device optimized for 4-THz operation. Since in both cases these access resistances are well below the real part of the source and load impedances ($\mathrm{Re}\{Z_s\} = 22.5\ \Omega$ for 2 THz and $\mathrm{Re}\{Z_s\} = 17.3\ \Omega$ for 4 THz, respectively), these parasitic resistances of the RTD-gated plasma wave HEMT can be considered to be part of the amplifier source resistance (i.e., they can be embedded into the source and load impedances computed with the model presented here).

It is worth noting that, in the above discussion, we have treated the access region as a lumped resistor instead of a transmission line, the ohmic contacts as perfect resistors, and the gate metal [forming an ohmic contact to the top n^+ GaN shown in Fig. 5(a)] to be lossless in the transmission line model. However, any media with a finite conductivity has its own characteristic high-frequency behavior, described by kinetic resistance, capacitance, and inductance. These effects need to be carefully modeled. For instance, Nishimura *et al.* has found that, using a cascaded transmission-line model, the gate fringing field over the access region effectively increases the device gate length, thus lowering the fundamental plasma frequency of the channel [28]. Employing the lumped element model, we observe that the parasitic resistance approaches the optimized source resistance at higher frequencies; beyond this point, the effects of parasitics with the assumed values

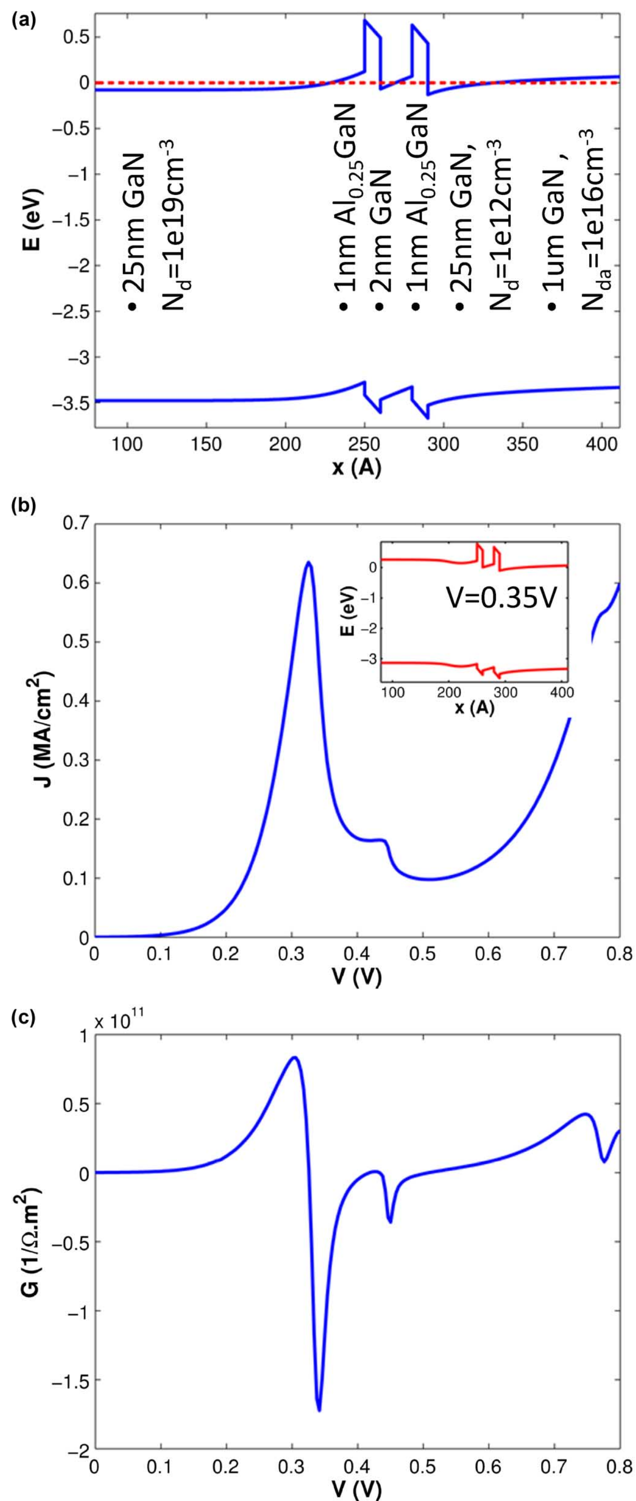

Fig. 5. GaN HEMT integrated with an RTD in the gate stack. (a) Heterostructure and energy band diagram at zero bias. (b) Calculated gate current as a function of gate voltage. (c) Differential conductance as a function of gate voltage.

above will prevent extrinsic power amplification even though the intrinsic RTD-gated plasma wave HEMT offers gain. As for reactive parasitics, the estimated parasitic capacitances are found to be more than 3× smaller than the device's intrinsic gate capacitance, as computed using self-consistent 1-D solutions to the Poisson–Schrodinger equations. Furthermore, the reactive component of the parasitics can be compensated for an optimized amplifier circuit through careful selection of embedding impedances. It should be noted that recent demonstrations of RTD-based emission near THz frequencies indicate that tunneling-induced negative conductance can be preserved well into the THz region [29]. As a result, experimental realization of THz power amplification in RTD-gated plasma wave HEMTs appears promising. Finally, we emphasize that though the material considered here is GaN, the RTD-gated plasma wave HEMT concept can in principle be extended to other material systems.

V. Conclusion

We have demonstrated the possibility of THz power amplification in HEMTs with gates exhibiting negative differential conductance. The fundamental mechanism enabling the gain is the interplay between the gate NDC and the plasma waves excited in the 2DEF. With suitable source and load impedances, a stable power gain (i.e. 5.2 dB at 2 THz, 4.8 dB at 4 THz) can be achieved in GaN-based RTD-gated plasma wave HEMTs.

References

[1] M. Tonouchi, "Cutting-edge terahertz technology," *Nature Photon.*, vol. 1, pp. 97–105, 2007.
[2] M. Dyakonov and M. S. Shur, "Shallow water analogy for a ballistic field effect transistor: New mechanism of plasma wave generation by dc current," *Phys. Rev. Lett.*, vol. 71, no. 15, pp. 2465–2468, 1993.
[3] M. Dyakonov and M. S. Shur, "Detection, mixing, and frequency multiplication of terahertz radiation by two-dimensional electronic fluid," *IEEE Trans. Electron Devices*, vol. 43, no. 3, pp. 380–387, 1996.
[4] R. Tauk, F. Teppe, S. Boubanga, D. Coquillat, W. Knap, Y. M. Meziani, C. Gallon, F. Boeuf, T. Skotnicki, C. Fenouillet-Beranger, D. K. Maude, S. Rumyantsev, and M. S. Shur, "Plasma wave detection of terahertz radiation by silicon field effects transistors: Responsivity and noise equivalent power," *Appl. Phys. Lett.*, vol. 89, no. 25, 2006, Art. ID 253511.
[5] A. V. Antonov, V. I. Gavrilenko, E. V. Demidov, S. V. Morozov, A. A. Dubinov, J. Lusakowski, W. Knap, N. Dyakonova, E. Kaminska, A. Piotrowska, K. Golaszewska, and M. S. Shur, "Electron transport and terahertz radiation detection in submicrometer-sized GaAs/AlGaAs field effect transistors with two-dimensional electron gas," *Phys. Solid State*, vol. 46, no. 1, pp. 146–149, 2004.
[6] T. Tanigawa, T. Onishi, S. Takigawa, and T. Otsuji, "Enhanced responsivity in a novel AlGaN/GaN plasmon-resonant terahertz detector using gate-dipole antenna with parasitic elements," in *Device Res. Conf. (DRC)*, 2010.
[7] W. Knap, J. Lusakowski, T. Parenty, S. Bollaert, A. Cappy, V. V. Popov, and M. S. Shur, "Terahertz emission by plasma waves in 60 nm gate high electron mobility transistors," *Appl. Phys. Lett*, vol. 84, pp. 2331–2333, 2004.
[8] S. Boubanga-Tombet, F. Teppe, J. Torres, A. El Moutaouakil, D. Coquillat, N. Dyakonova, C. Consejo, P. Arcade, P. Nouvel, H. Marinchio, T. Laurent, C. Palermo, A. Penarier, T. Otsuji, L. Varani, and W. Knap, "Room temperature coherent and voltage tunable terahertz emission from nanometer-sized field effect transistors," *Appl. Phys. Lett.*, vol. 97, 2010, Art. ID 262108.
[9] W. Knap, V. Kachorovskii, Y. Deng, S. Rumyantsev, J.-Q. Lu, R. Gaska, M. S. Shur, G. Simin, X. Hu, M. A. Khan, C. A. Saylor, and L. C. Brunel, "Nonresonant detection of terahertz radiation in field effect transistors," *J. Appl. Phys.*, vol. 91, no. 11, pp. 9346–9353, 2002.
[10] B. Sensale-Rodriguez, L. Liu, R. Wang, D. Jena, and H. G. Xing, "FET THz Detectors operating in the quantum capacitance limited region," *Int. J. High Speed Electron. Syst.*, vol. 20, no. 3, pp. 597–609, 2011.
[11] V. Ryzhii, I. Khmyrova, and M. Shur, "Resonant detection and frequency multiplication of terahertz radiation utilizing plasma waves in resonant-tunneling transistors," *J. Appl. Phys.*, vol. 88, no. 5, pp. 2868–2871, 2000.
[12] V. Ryzhii and M. Shur, "Plasma instability and nonlinear terahertz oscillations in resonant-tunneling structures," *Jpn. J. Appl. Phys.*, vol. 40, pp. 546–550, 2001.
[13] B. Sensale-Rodriguez, P. Fay, L. Liu, D. Jena, and H. G. Xing, "Enhanced Terahertz detection in resonant tunnel diode-gated HEMTs," *ECS Trans.*, vol. 49, no. 1, pp. 93–102, 2012.
[14] T. Fang, R. Wang, H. Xing, S. Rajan, and D. Jena, "Effect of optical phonon scattering on the performance of GaN transistors," *IEEE Electron Device Lett.*, vol. 33, no. 5, pp. 709–711, May 2012.
[15] P. Burke, I. Spielman, J. Eisenstein, L. Pfeiffer, and K. West, "High frequency conductivity of the high-mobility two-dimensional electron gas," *Appl. Phys. Lett.*, vol. 76, pp. 745–747, 2000.
[16] I. Khmyrova and Y. Seijyou, "Analysis of plasma oscillations in high-electron mobility transistor like structures: Distributed circuit approach," *Appl. Phys. Lett.*, vol. 91, 2007, Art. ID 143515.
[17] F. Capasso, S. Sen, and A. Cho, "Negative transconductance resonant tunneling field effect transistor," *Appl. Phys. Lett.*, vol. 51, pp. 526–528, 1987.
[18] D. M. Pozar, *Microwave Engineering*, 3rd ed. New York: Wiley, 2004.
[19] R. H. Byrd, J. C. Gilbert, and J. Nocedal, "A trust region method based on interior point techniques for nonlinear programming," *Math. Program.*, vol. 89, no. 1, pp. 149–185, 2000.
[20] M. Olivieri, G. Scotti, P. Tommasino, and A. Trifiletti, "Necessary and sufficient conditions for the stability of microwave amplifiers with variable termination impedances," *IEEE Trans. Microw. Theory Tech.*, vol. 53, no. 8, p. 2580, Aug. 2005.
[21] Y. Cao, K. Wang, A. Orlov, H. Xing, and D. Jena, "Very low sheet resistance and Shubnikov-de-Haas oscillations in two-dimensional electron gases at ultrathin binary AlN/GaN heterojunctions," *Appl. Phys. Lett.*, vol. 92, 2008, Art. ID 152112.
[22] E. L. Ginzton, W. R. Hewlett, J. H. Jasberg, and J. D. Noe, "Distributed amplification," in *Proc. IRE*, 1948, vol. 36, pp. 956–969.
[23] I.-H. Tan, G. L. Snider, and E. L. Hu, "A self-consistent solution of Schrödinger–Poisson equations using a nonuniform mesh," *J. Appl. Phys.*, vol. 68, pp. 4071–4076, 1990.
[24] H. Mizuta and T. Tanoue, *The Physics and Applications of Resonant Tunneling Diodes*. Cambridge, U.K.: Cambridge Univ., 1995.
[25] N. Shimizu, T. Waho, and T. Ishibashi, "Capacitance anomaly in the negative differential region of resonant tunneling diodes," *Jpn. J. Appl. Phys.*, vol. 36, pp. L330–L333, 1997.
[26] K. Shinohara, D. Regan, A. L. Corrion, D. Brown, S. D. Burnham, P. J. Willadsen, I. Alvarado-Rodriguez, M. Cunningham, C. M. Butler, A. Schmitz, S. Kim, B. Holden, D. Chang, V. Lee, A. Ohoka, P. M. Asbeck, and M. Micovic, "Deeply-scaled self-aligned-gate GaN DH-HEMTs with ultrahigh cutoff frequency," in *IEDM Tech. Dig.*, 2011, p. 19.1.1.
[27] J. Guo, G. Li, F. Faria, Y. Cao, R. Wang, J. Verma, X. Gao, S. Guo, E. Beam, A. Ketterson, M. Schuette, P. Saunier, M. Wistey, D. Jena, and H. G. Xing, "MBE regrown ohmics in InAlN HEMTs with a regrowth interface resistance of 0.05 ohm-mm," *IEEE Electron Device Lett.*, vol. 33, no. 4, pp. 525–527, Apr. 2012.
[28] T. Nishimura, N. Magome, I. Khmyrova, T. Suemitsu, W. Knap, and T. Otsuji, "Analysis of fringing effect on resonant plasma frequency in plasma wave devices," *Jpn. J. Appl. Phys.*, vol. 48, 2009, Art. ID 04C096.
[29] M. Feiginov, C. Sydlo, O. Cojocari, and P. Meissner, "Resonant-tunnelling-diode oscillators operating at frequencies above 1.1 THz," *Appl. Phys. Lett.*, vol. 99, no. 23, 2011, Art. ID 233506.

Berardi Sensale-Rodríguez (S'07) received the Engineer's degree from Universidad de la República, Uruguay, in 2008. He is currently working toward the Ph.D. degree in electrical engineering at the University of Notre Dame, Notre Dame, IN, USA.

His early research interests were focused on numerical modeling of RF/microwave components and analog circuit design oriented towards low-power (subthreshold) portable and implantable electronics. His research at the University of Notre Dame has been focused on the proposal and development of novel THz devices and systems. More recent interests include optoelectronic

devices. He has authored and coauthored over 30 research papers in these and related areas.

Mr. Sensale-Rodríguez is a member of the International Society for Optical Engineers and the American Physical Society and an associate member of the Uruguayan National Researchers System (SNI). He was the recipient of the Best Student Paper Award from IRMMW-THz 2012.

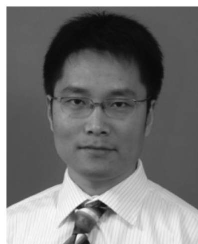

Lei Liu (S'99–M'07) received the B.S. and M.S. degrees from Nanjing University, Nanjing, China, in 1998 and 2001, respectively, and the Ph.D. degree from the University of Virginia, Charlottesville, VA, USA, in 2007, all in electrical engineering.

From 2007 to 2009, he was a Post-Doctoral Research Associate with the Department of Electrical and Computer Engineering, University of Virginia, Charlottesville, VA, USA. In September 2009, he joined the faculty of the University of Notre Dame, Notre Dame, IN, USA, where he is now an Assistant Professor of electrical engineering. His research interests include millimeter- and submillimeter-wave device and circuit design, modeling, and testing, quasi-optical techniques, terahertz detectors for imaging and spectroscopy, novel microwave materials and devices, superconducting electronics, microfabrication and processing.

Patrick Fay (M'99–SM'07) received the B.S. degree from the University of Notre Dame, Notre Dame, IN, USA, in 1991, and the Ph.D. degree from the University of Illinois at Urbana-Champaign, Urbana, IL, USA, in 1996, both in electrical engineering.

He is currently a Professor with the Department of Electrical Engineering, University of Notre Dame, Notre Dame, IN, USA. He served as a Visiting Assistant Professor with the Department of Electrical and Computer Engineering, University of Illinois at Urbana-Champaign, Urbana, IL, USA, in 1996 and 1997, and joined the faculty at the University of Notre Dame in 1997. He has authored and coauthored eight book chapters and more than 90 articles in refereed scientific journals. His research interests include the design, fabrication, and characterization of microwave and millimeter-wave electronic devices and circuits, as well as high-speed optoelectronic devices and optoelectronic integrated circuits for fiber optic telecommunications. His research also includes the development and use of micromachining techniques for the fabrication of microwave components and packaging. His educational initiatives include the development of an advanced undergraduate laboratory course in microwave circuit design and characterization, and graduate courses in optoelectronic devices and electronic device characterization.

Dr. Fay was the recipient of the Department of Electrical Engineering's IEEE Outstanding Teacher Award in 1998–1999.

Debdeep Jena (M'03) received the B.Tech. degree in electrical engineering from the Indian Institute of Technology, Kanpur, India, in 1998, and the Ph.D. degree in electrical and computer engineering from the University of California, Santa Barbara, CA, USA, in 2003.

Since 2003, he has been with the faculty of the Department of Electrical Engineering, University of Notre Dame, Notre Dame, IN, USA. His research and teaching interests are in the MBE growth and device applications of quantum semiconductor heterostructures (currently III–V nitride semiconductors), investigation of charge transport in nanostructured semiconducting materials such as graphene, nanowires, and nanocrystals, and their device applications, and in the theory of charge, heat, and spin transport in nanomaterials.

Dr. Jena was the recipient of several awards, including two Best Student Paper Awards in 2000 and 2002 for his Ph.D. dissertation research, the National Science Foundation CAREER Award in 2007, the Joyce Award for excellence in undergraduate teaching in 2010, the ISCS Young Scientist, and an IBM Faculty Award in 2012.

Huili Grace Xing (S'01–M'03) received the B.S. degree in physics from Peking University, Beijing, China, in 1996, the M.S. degree in material science from Lehigh University, Bethlehem, PA, USA, in 1998, and the Ph.D. degree in electrical engineering from the University of California, Santa Barbara, CA, USA, in 2003.

She is currently the John Cardinal O'Hara CSC Associate Professor of Electrical Engineering at the University of Notre Dame, Notre Dame, IN, USA. Her research focuses on development of III–V nitride and 2-D crystal semiconductor growth and (opto)electronic devices, especially the interplay between the material properties and device developments. More recent research interests include THz applications.

Dr. Xing was the recipient of an AFOSR Young Investigator Award and an NSF CAREER Award.